Evaluation of Al/SiC Wetting Characteristics in Functionally Graded Metal-Matrix Composites by Synchrotron Radiation Microtomography

A. Velhinho [(*) 1, 2] , P.D. Sequeira [3], Rui Martins [1], G. Vignoles [5],

F. Braz Fernandes [1,2], J.D. Botas [2], L.A. Rocha [3, 4]

[1] CENIMAT - Centro de Investigação em Materiais, Universidade Nova de Lisboa, Faculdade de Ciências e Tecnologia, Universidade Nova de Lisboa, Quinta da Torre, 2829-516 Caparica – PORTUGAL

[2] DCM - Departamento de Ciência dos Materiais, Universidade Nova de Lisboa, Faculdade de Ciências e Tecnologia, Universidade Nova de Lisboa, Quinta da Torre, 2829-516 Caparica – PORTUGAL

[3] CIICS – Centro de Investigação em Comportamento de Superfícies, Universidade do Minho, Campus de Gualtar, 4800-058 Guimarães PORTUGAL

[4] DEM –Departamento de Engenharia Mecânica, Universidade do Minho, Campus de Gualtar, 4800-058 Guimarães PORTUGAL

[5] LCTS – Laboratoire des Composites Thermostructuraux, Université de Bordeaux 1, Domaine Universitaire – 3, Allée de la Boétie – 33600 Pessac FRANCE

Keywords: Metal matrix composites, Functionally graded materials, Centrifugal casting, syncrothron radiation, X-ray microtomography.

Abstract. The concept of functionally graded material (FGM), may be considered as a model particularly interesting to be applied in components for the automotive industry, if reliability and cost can be controlled in an advantageous way. In fact, coupling superior superficial wear resistance with a significant bulk toughness, without compromising important weight savings, by using Al-Si metal matrix composites (MMC's) selectively reinforced at the surface with SiC particles, is likely to be considered as a innovative advance to that industrial field, if adequate production techniques are developed. Casting under a centrifugal force may well be considered as one of the most effective methods for processing Al-based FGM´s. A primary problem to be faced when producing MMC´s reinforced with ceramic particles is related with the imperfect wetting of the ceramic particles by the molten matrix alloy. A first consequence of defective wetting may be the formation of ceramic-ceramic, ceramic-gas and/or metal-gas interfaces, instead of the desired metal-ceramic interface. Secondly, wetting phenomena play an essential role regarding the physical, chemical and mechanical characteristics of the metal/ceramic interface. A general consequence of these aspects may be related with the degradation of the material properties, be it mechanical, chemical, or thermal in nature. The present work refers to an X-ray microtomography experiment aiming at the elucidation of some aspects regarding particle distribution in SiC_p-reinforced functionally graded aluminium composites. Precursor composites were produced by rheocasting. These were then molten and centrifugally cast in order to produce the FGM composites. From these, small cylindrical samples were extracted and observed by X-ray microtomography at the European Synchrotron Radiation Facility (ESRF). The 3D tomographic images were obtained in edge-detection mode (phase-contrast mode), and an adequate segmentation procedure was employed to isolate the pores and SiC particles from the Al matrix. This has allowed a study of the relations between the matrix, the SiC particles, and locally intervening porosities of varying shapes, aiming at a better understanding of the mechanisms involved.

Introduction

The relevance of the spatial distribution of the reinforcement in a MMC, and of the interaction between ceramic particles and metallic matrix is, already great in conventional MMC's, becomes utterly significant in functionally graded materials (FGM's), namely due to its implication in failure processes [1].

Complete understanding of the phenomena governing the distribution of the particles and of the mechanisms leading to their distribution has not yet been achieved [2]. Further complication arises from the presence of voids and pores within the material. Porosity can have different causes and, depending on its origin, may exhibit differing morphologies. Nevertheless, it will invariably contribute to microstructural inhomogeneity and will affect the particle distribution.

One contribution to porosity stems from the presence of gases dissolved in the metallic melt during casting. This kind of porosity generally reveals itself as small bubbles (known as micropores), which arise from a decrease in the solubility of the gas (usually hydrogen) in liquid and solid aluminium during cooling [3].

Moreover, in the case of cast MMC's, a further source of gas intervenes, in the form of gas entrained into the slurry during mixing, to which the ceramic particles tend to become attached [4].

A further contribution to porosity consists in solidification shrinkage of the matrix [4].

Finally, voids within the MMC may also result from particle clusters, which may form a barrier to the penetration of liquid, thus preventing wetting of the sheltered ceramic surfaces by the metal.

Although not all the pores present in a MMC do contact with the particles, quantification of the fraction that does assumes relevance, since it represents less than satisfactory particle/matrix interface characteristics.

Even if conventional techniques based on 2-D metallography provide useful estimators for important parameters like particle size distribution [5, 6] and particle volume fraction [5-11], some 3-D stereological parameters, namely connectivity [12], are beyond its reach. Such parameters can only be assessed directly by techniques where the 3-dimensional nature is an intrinsic characteristic, as is the case of tomography. Moreover, the features under evaluation, by their scale, demand spatial resolutions in the order of 10 μm or less, thus leading to the use of X-ray microtomography with synchrotron radiation.

Experimental procedure

A precursor conventional MMC was prepared from a commercial AS7G03 (Al 7 Si 0,3 Mg) alloy and SiC particles were produced by rheocasting. A Coulter LS230 laser interpherometer was used to determine size distribution of the SiC particles added to the melt. Median grain size of SiC particles was 37.4 mm.

The MMC was then molten and centrifugally cast using a Linn High Therm Titancast 700 μP Vac furnace, in order to obtain the functionally graded composites.

Details of both processes are available elsewhere [13-18].

From the FGM, cylindrical samples, around 1 mm in diameter, were machined by EDM. The axis of each sample was parallel to the direction of the functional gradient. The original positions of the samples defined a regular grid.

The samples were analysed by X-ray microtomography at the ID 19 beamline of the European Synchrotron Radiation Facility, in Grenoble.

Several Regions of Interest (ROI) were scanned along each sample. Our attention in the present work will be devoted to a single sub-set from a specific representative ROI located at 13 mm from the surface of a sample extracted close to the longitudinal axis of the FGM composite. This particular dataset shall henceforward be designated as VOI (Volume of Interest).

The microtomography measurements were performed using a beam energy of 20 keV, employing a multilayer as monochromator. The sample was placed at 100 mm from the detector, a FRELON

1024*1024 CCD camera. This distance gave access to edge detection mode in order to enhance contrast between SiC particles and aluminium matrix. Pixel size was 0.95 μm.

Even though the experiments were conducted in phase-contrast mode, X-ray absorption contrast between the matrix and the reinforcing particles was still too weak to allow easy image segmentation. It became thus necessary to evolve an adequate image segmentation procedure further treatment, with the use of a modified version of an algorithm previously developed at LCTS [19]. Detailed treatment of that procedure pertains to a previously published work [18].

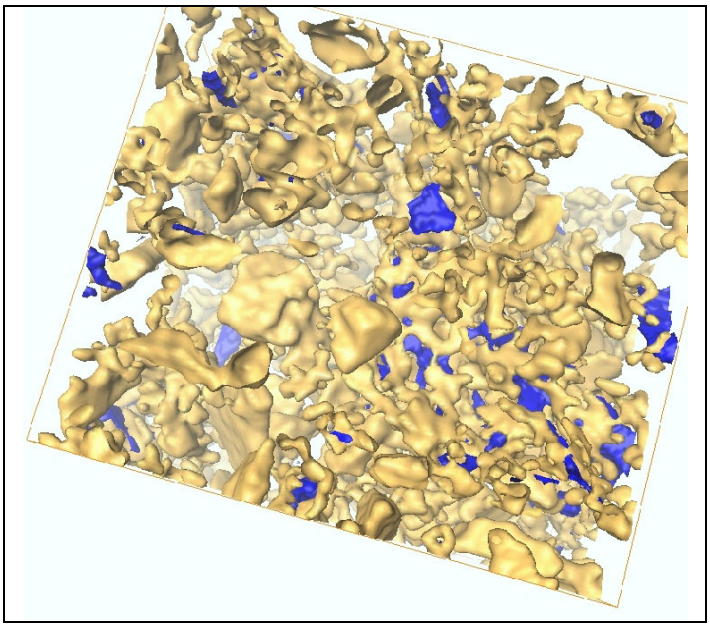

Figure 1 – Reconstructed tomographic image of a 200 x 200 x 200 voxels (0.19^3 μm^3) VOI, showing the reinforcing SiC particles, in yellow, and revealing the presence of porosity, in blue.

Results and Discussion

The overall particle content within the VOI of concern, as determined by X-ray microtomography, corresponded to 16.0 vol.%, while the overall porosity content was 0.8 vol.% [18].

As shown in the reconstructed tomographic image in Fig. 1, three distinct phases can be distinguished in the VOI: apart from the Al matrix and the SiC reinforcements, a number of porosities are present. Fig. 2 presents a reconstructed image of some pores found in the VOI. Careful observation of both images reveals variations in pore size and shape, as well as different types of interactions between pores and ceramic particles, deserving more detailed consideration.

Since we are dealing with three-dimensional objects, any relevant form of quantifying its shape must take volume into account. One simple way of doing this involves de definition, for each object, of a bounding box, i.e., a parallelepiped whose edge length is the same as the measured maximum sizes of the particle along the three axes of the reconstructed VOI. It then becomes possible to calculate a shape factor ψ simply by dividing the bounding box volume by the object reconstructed volume. Although this ratio varies with object misalignment relative to the VOI axis (a parallelepiped object shows a unitary shape factor only when it is aligned with the VOI axis), it can nevertheless be of use when dealing with a large number of objects, provided those objects are not excessively elongated in shape and do not exhibit any preferred orientation, since it is simple to compute.

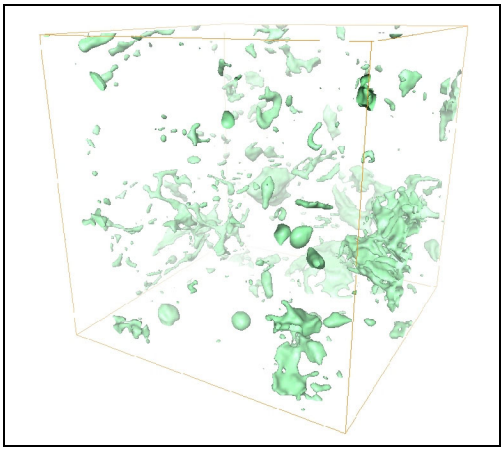

Figure 2 – Another reconstructed tomographic image of a 200 x 200 x 200 voxels (0.19^3 μm^3) VOI, this time showing some of the pores occurring in the material, but omitting visualisation of the SiC particles.

Fig. 3 shows the correspondence between the pore shape factor and the pore volume. This shows a large number of pores with $\psi \approx 2\text{-}3$, corresponding to eminently round pores, with little ramifications ($\psi = \frac{6}{\pi} = 1.91$ for a sphere), but shows also that the lesser number of intricate pores can not be overlooked, due to the importance of their volume, and the resulting high probability of being in contact with SiC

particles. This information must be complemented with the pore shape distribution, presented in Fig. 4, confirming that the great majority of the pore population consists of round pores.

Computation of the average number of pore/particle contacts per pore as a function of the pore shape factor yields the result also shown in Fig. 4. It ensues that on average only those particles of high ψ, i.e., exhibiting a very complex shape, participate in multiple contacts, whereas the remaining pore population generally contact no more than one particle at most.

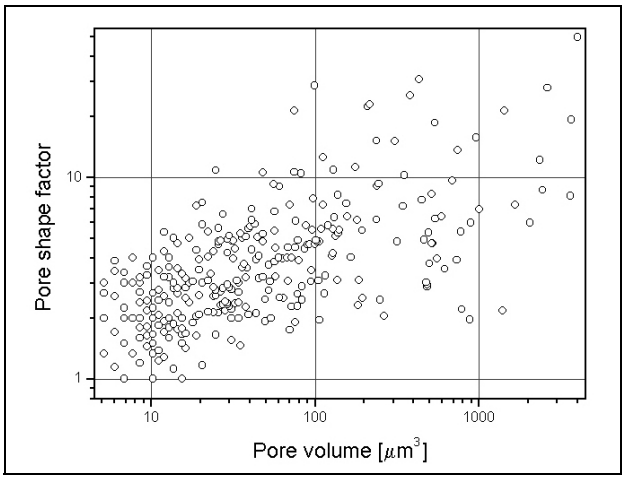

Figure 3 – Pore shape factor plotted against the volume of the pores.

Conversely, Fig. 4 also presents results of a similar computation for the particles contacted by pores of a given shape factor, showing that the number of pores touching each contacted particle decreases with increasing ψ value; while in the case of round pores several of these surround each contacted particle, for complex pores each particle is touched, on average, by approximately no more than one pore, as if it is partially surrounded by it.

In Fig. 5 the fraction of pores with a given ψ effectively contacting particles is presented. It can be seen that, except for the most complex-shaped cases, at least one-quarter to one-third of the pores present in the VOI do not participate in any contact.

Likewise, when reported to the overall particle population, the fraction of particles touched by pores of a given shape factor is relatively small (between 0.01 and 0.14), with the highest proportions corresponding to round pores (generally small but present in great numbers) and to very complex pores (few in number, but very extensive). Nevertheless, the presence of porosity represents a powerful limiting factor to the establishment of proper metal/ceramic interfaces, since the accumulated fraction of particles contacting any sort of pore stands at 0.70, meaning that 7 out of every 10 SiC particles present a metal/ceramic interface disturbed by porosity.

The tendencies illustrated by Figs. 3, 4 and 5 suggest that the pores presenting small ψ values effectively correspond to the presence of gases in the melt, either dissolved in the matrix, or entrained into the material by agitation; these pores would show some tendency to nucleate near the ceramic particles, but this tendency would not be exclusive, with almost half affecting solely the aluminium matrix.

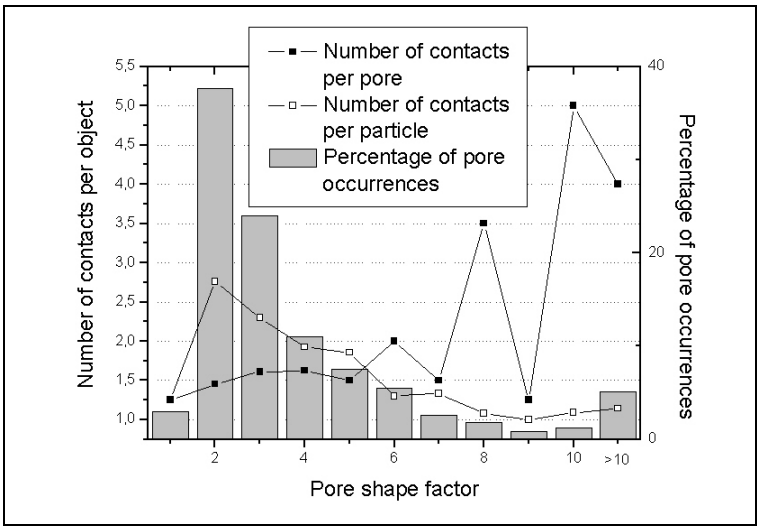

Figure 4 – The figure correlates the pore shape distribution, as the number of pore occurrences for each pore shape factor class, with the number of contacts per pore effectively touching one or more particles, and with the number of contacts per particle effectively touched by pores of that class.

On the opposite end of the ψ range the small minority of very complex-shaped and extensive pores would pertain to spaces left vacant by liquid due to the presence of particle clusters.

In between remains a population of pores of intermediate ψ value which, its complex shape notwithstanding, contact but a small number of particles each. This behaviour suggests that these pores are essentially due to solidification shrinkage of the matrix. Since solidification shrinkage occurs preferentially along matrix grain

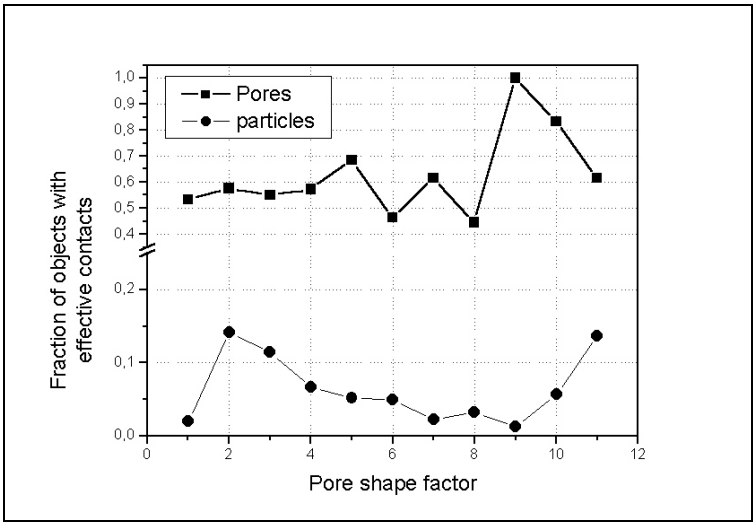

Figure 5 – Fractions of pores (reported to the number of pores of the same pore shape factor class) and of particles (reported to the overall particle population) effectively participating in pore/shape contacts, as a function of pore shape factor.

boundaries, the resulting number of particles contacted would tend to remain relatively low.

The plots included in Fig. 6 are two examples representing the centroid positions of pores within a given interval of ψ values effectively contacting particles, and those of the corresponding particles. Although exact determination of neighbouring relations is excluded, this kind of representation, through the omission of information about the volume and contour of each individual object, provides a way of easily visualising the pore and particle populations maintaining contact of a given type, and thus of assessing the spatial distribution and density of that class of contacts throughout the VOI.

Observing the plots, it can be seen that, in the case of lower ψ (Fig. 6a)), particles and pores seem to occupy positions equally distributed all over the VOI, whereas for higher ψ (Fig. 6b)) the spatial dispersion of the centroids of contacted particles is much wider than that of the pore centroids themselves, with at least some of the pores surrounded by "clouds" of particles, a further indication of the fact that pores in this class of ψ, apart from being extensive and far-reaching, are related to groups of particles in close vicinity, as is the case when SiC particles form clusters.

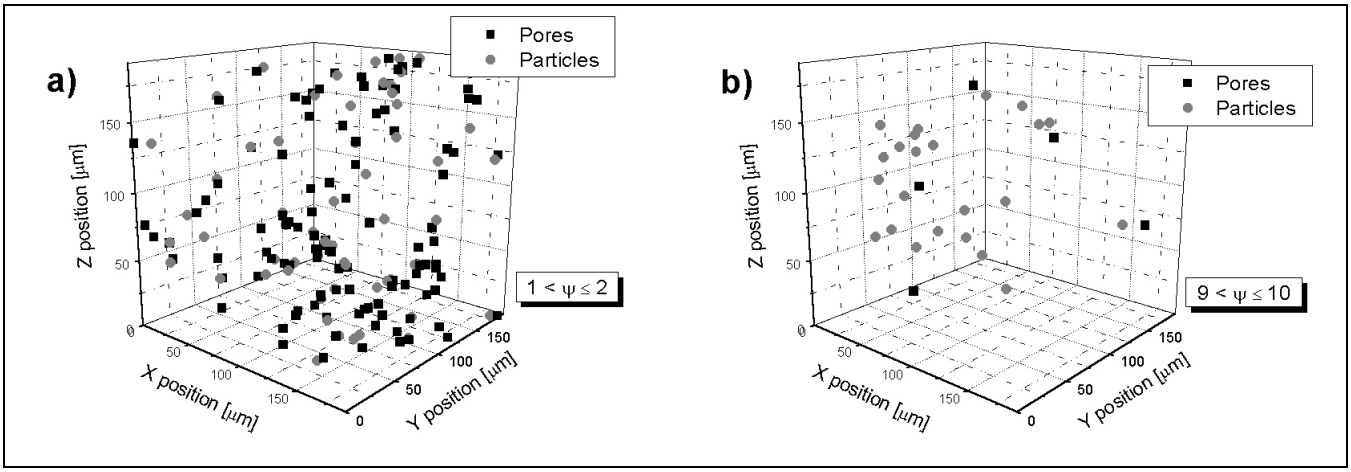

Figure 6 – Three-dimensional plots representing the populations of pores and particles in contact with each other for a given interval of ψ values. Each object is represented through the position of its centroid, contour representation being omitted. a) $1 < \psi \leq 2$; b) $9 < \psi \leq 10$.

Conclusions

In this work we explored results obtained from synchrotron radiation X-ray microtomography to study the disruption caused in the formation of sound Al/SiC interfaces, in a FGM Al-matrix SiC_p-reinforced, by different types of porosities, characterized by differing shapes.

It was found that the presence of all kinds of pores seriously disrupts the formation of the metal/ceramic interfaces, by affecting 70% of the SiC particles present in the VOI. Most of the particles thus affected are in contact with gas bubbles, either formed due to decreases in the solubility of the melt

during solidification, or consisting of gases entrained by agitation of the slurry during processing.

A second important source of hindrance to the establishment of the Al/SiC interface stems from the presence of particle clusters, acting during solidification as barriers to the penetration of liquid aluminium.

Finally, a third source of porosity in the material is solidification shrinkage, whose relevance to the disturbance of metal/ceramic interfaces is secondary, since it predominantly regards the aluminium matrix.

References

[1] – T.W. Clyne, P.W. Withers, "An Introduction to Metal Matrix Composites", E.A. Davis, I.M. Ward FRS (Eds.), CUP, Cambridge 1993, 510 pp.

[2] – Y. Watanabe, N. Yamanaka, Y. Fukui, Composites Part A, 29A (1998) pp. 595-601

[3] – J. Anson, R. Drew, J. Gruzleski, Met. and Mat. Trans. B, 30B (1999) pp. 1027-1033

[4] – G. Hanumanth, G. Irons, Proc. Fabr. Part. Reinf. Met. Comp.(1990) pp. 41-46

[5] – L.A. Rocha, A.E. Dias, D. Soares, C.M. Sá, A.C. Ferro, Ceramic Transactions, 114 (2001) pp. 467-474

[6] – L. A. Rocha, P. D. Sequeira, A. Velhinho, C. M. Sá, XVI Congresso Brasileiro de Engenharia Mecânica (2001) pp. 381-388

[7] – L. Lajoye, M. Suéry, Proc. Int. Symp. on Advances in Cast Reinforced Metal Composites, (1988) ed. ASM International, pp. 15-20

[8] – Y. Watanabe, Y. Fukui, Recent Res. Devel. Metallurg. & Materials Sci., 4 (2000) pp. 51-93

[9] – Y. Watanabe, Y. Fukui, Aluminum Transactions, 2 (2000) pp. 195-208

[10] – A. Ourdjini, K.C. Chew, B.T. Hhoo, J. Mat. Proc. Technol., 116 (2001) pp. 72-76

[11] – R. Rodríguez-Castro, R.C. Wetherhold, M.H. Kelestemur, Mat. Sci. & Eng. A, A323 (2002) pp. 445-456

[12] - J.-M. Chaix, Journées d'Automne 2001 de la Société Française de Métallurgie et de Matériaux, Paris (2001), p. 80

[13] – C. Ferreira, J. Teixeira, J. D. Botas, Proc. 8º Encontro da Soc. Portuguesa de Materiais (1997), pp. 9-18

[14] – C. Ferreira, "Processos Tecnológicos Associados è Reo-Fundição", PhD Thesis, Universidade Nova de Lisboa (1999) 305 pp.

[15] – A. Velhinho, F.M. Braz Fernandes, J.D. Botas, Key Eng. Mat. Vol. 230-232 (2002), pp. 226-230

[16] – L.A. Rocha, A.E. Dias, D. Soares, C.M. Sá, A.C. Ferro, Ceramic Transactions, 114 (2001) pp. 467-474

[17] – L. A. Rocha, P. D. Sequeira, A. Velhinho, C. M. Sá, XVI Congresso Brasileiro de Engenharia Mecânica (2001) pp. 381-388

[18] – A. Velhinho, P.D. Sequeira, Rui Martins, G. Vignoles, F.M. Braz Fernandes, J.D. Botas, L.A. Rocha, E-MRS Spring Meeting 2002 (France 2002); accepted for publication by Nuclear Instr. & Methods in Phys. B

[19] – G. Vignoles, Carbon, 39 (2001) pp. 167-173

Acknowledgements

The authors wish to acknowledge E. Boller and P. Cloetens, as well as all the remaining staff at ESRF, for their assistance and cooperation during the microtomography experiments.

The financial support obtained by A. Velhinho from Fundo Social Europeu, under the program PRODEP, is gratefully acknowledged. Part of the work was supported by Fundação para a Ciência e Tecnologia (FCT - Portugal), under contract POCTI/12301/2001.